PAPER • OPEN ACCESS

Influence of PVA resin and cross-linking agent on the structure and properties of semi-refined carrageenan-based packaging films

To cite this article: S Zhang *et al* 2024 *J. Phys.: Conf. Ser.* **2680** 012006

View the article online for updates and enhancements.

Influence of PVA resin and cross-linking agent on the structure and properties of semi-refined carrageenan-based packaging films

S Zhang[1], H G Guo[1,*], M J Cran[2]

[1] Faculty of Light Industry, Qilu University of Technology, Jinan 250353, China
[2] Institute for Sustainable Industries and Liveable Cities, Victoria University, PO Box 14428, Melbourne 8001, Australia

*E-mail: ghg@qlu.edu.cn

Abstract. For the high content of carrageenan in some seaweed and the low cost and easy availability of semi refined carrageenan (SRC), SRC resin powder was selected as our research object. Due to its water solubility, a solution casting method was adopted to form film, hoping to prepare food packaging materials that partially replace petroleum based resin. The pure SRC resin casting film is very brittle and cannot be formed. Therefore, 40wt% glycerol was added to the formula to plasticize and improve the flexibility and demoulding ability of SRC. The plasticized SRC film still has limitations. Soluble petroleum based polymer poly(vinyl alcohol) (PVA) resin was used as a blending modifier, cinnamaldehyde (CIN) as a crosslinking agent for acetal reaction with hydroxyl groups, boric acid (BA) as a provider of acidic environment and an auxiliary agent for generating partial hydrogen bonds with hydroxyl groups. Eight experimental research formulas were designed and FTIR, XRD, thermodynamic properties and mechanical properties of the modified films were analyzed. Both microscopic and macroscopic analyses have shown that under the acidic conditions of BA, CIN undergoes an acetal reaction with SRC and PVA, therefore mass ratio of the formula that SRC/glycerol/PVA/CIN/BA is 100/40/33.3/10/10, the film has the best tensile strength of 34.85Mpa, higher than that of other films. It has been proven that CIN does indeed act as a crosslinking agent in the formula, forming a network structure that enhances it.

1. Introduction

Carrageenan is one of the polymers that can be obtained by extraction from certain species of seaweeds such as Eucheuma cottonii. It consists of α-(1-3)-D-galactose and β-(1-4)-3,6-anhydro-D- or L-galactose alternatively co-polymerized as a water-soluble sulfated linear polysaccharide [1]. These sulfate groups on the disaccharide repeating unit determine the classification into one of three major carrageenan types: lambda (λ), kappa (κ), and iota (ι) as depicted in Figure 1 [2]. It is becoming increasingly recognizable as a novel and promising candidate of renewable biomaterial for that is a substitute for the conventional synthetic plastics. Its renewable, biodegradable, good biocompatibility and film-forming properties, allowing the production of biodegradable films or hydrogels for food packaging and biomedical applications [3]. The production of petroleum-based films is dependent on petroleum resources, which are becoming increasingly scarce over time [4, 5]. The purpose is to prepare a blend film to reduce the cost of PVA films Secondly, forming a co-crosslinking structure through acetal reaction with hydroxyl group of PVA and carrageenan, improving the compatibility of the film, and thereby improving water

resistance and mechanical properties. Carrageenan casting film has great advantages over traditional petroleum-based film. Solution cast method is a common method for film production [6]. This method involves the preparation of the film-forming solution, spreading the prepared solution on a mold made of glass plates and evaporating the solvent after cooling [7]. This method has the advantages of low cost and simplicity of operation [8]. And PVA resin melt processing difficulties, cast into the film using water as a solvent, which solves the problem of processing is also more environmentally friendly. Carrageenan is extracted from natural resources such as seaweed and is renewable. It can be decomposed by microorganisms in the natural environment and eventually converted into CO_2 and H_2O, which makes carrageenan-based films more environmentally friendly [9].

(a) λ-carrageenan   (b) κ-carrageenan   (c) ι-carrageenan
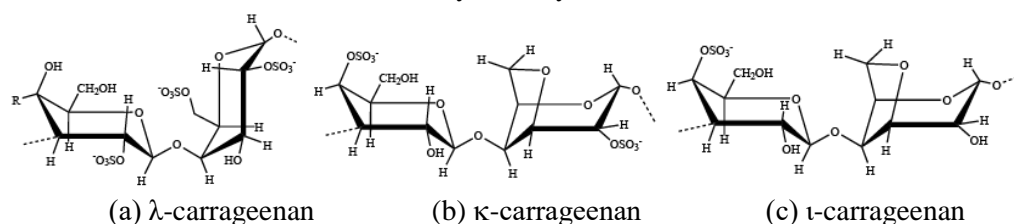
Figure 1. Chemical structure of carrageenans

Daei [10] et al. added red beet extract and plantain gum to the blend, the film gained improved antioxidant performance and shortened biodegradation time. However, the lack of desired mechanical, thermal and water solubility of carrageenan has resulted in the limited application in the food packaging industry [11]. To overcome these limitations, reinforcing agent and crosslinker are incorporated into biopolymer films [12].

Petroleum-based resin poly (vinyl alcohol) (PVA) is widely used in the manufacture of packaging film due to its good film-forming property, optical transparency, gas barrier and mechanical properties. It is readily consumed by microorganisms and enzymes when exposed to natural environment. PVA is suitable to be used as biodegradable packaging materials to reduce accumulation of synthetic petroleum-based polymer solid wastes. PVA films have better gas barrier properties, effectively isolating the permeation of oxygen and other gases. This is important for protecting food and other products that are susceptible to oxidation, and PVA films have better barrier properties than polyethylene (PE) films, providing a better barrier to oxygen. PVA films have better light transmission than polypropylene (PP) films, making packaged products more attractive. But the price of PVA is quite expensive [13]. In order to make PVA more economical to use, a small ratio of PVA can be added into carrageenan. Carrageenan possesses similar functionality as PVA which is biocompatible and consumable by microorganisms as well [14-16]. Bajpai [17] studied the hygroscopic behavior and water vapor permeability of glutaraldehyde cross-linked carrageenan/ polyvinyl alcohol films. The moisture permeation study reveals that carrageenan/ polyvinyl films are suitable for the wounds which are having low exudates. When PVA and carrageenan are blended together [18], the presence of hydroxyl groups (–OH) tend to form strong hydrogen bonding among the molecules and subsequently lead to synergistic stability and better system integrity to improve the mechanical property, as showed in Figure 2.
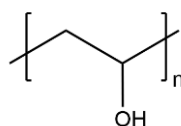
Figure 2. Chemical structure of PVA

In order to make the film more hydrophobic, aldehyde compounds were introduced into the blend. Cinnamaldehyde (CIN) is a phenylpropanoid that is naturally synthesized by the shikimate pathway [19]. This pale yellow, viscous liquid occurs in the bark of cinnamon trees and other species of the genus Cinnamomum. There are two isomers of CIN, cis and trans isomers. At present, the natural

CIN found in nature exists in trans structures showed in Figure 3. CIN's aldehyde end group may react with the hydroxyl of Carrageenan and PVA in acidic environment as showed in Figure 4 [20].
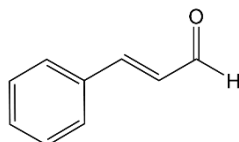
Figure 3. Chemical structure of CIN
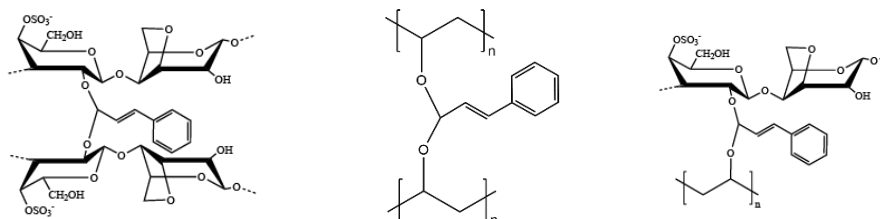
(a) Acetal reaction products with carrageenan   (b) with PVA   (c) with carrageenan and PVA

Figure 4. Acetal reaction products of CIN

Boric acid (BA) was considered to provide the acidic environment and was another crosslinker of PVA showed in Figure 5.
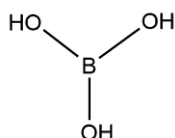
Figure 5. Chemical structure of BA

Under certain conditions, BA exhibits a rather strong interaction with PVA, leading to a rapid precipitation of the polymer complex from the solution [21]. This gives us reason to assume that their interaction is a chemical bond (Figure 6 a). Another concept refers to the H-bond between BA and PVA (Figure 6b) [22]. Recently, a third structure has been proposed, which represents a hybrid interpolymeric complex (Figure 6 c) [23].
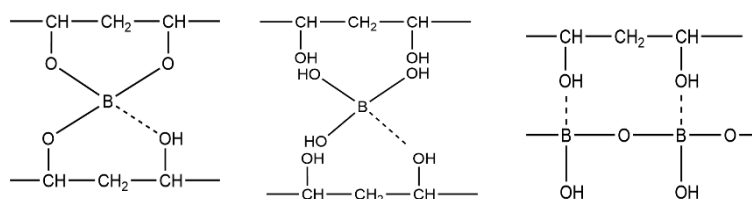
(a) chemical bonding   (b) H- bonding   (c) a hybrid inter polymeric complex

Figure 6. Suggested structures of PVA-BA complex

It appeared that the water resistance, oxygen resistance, thermal stability and mechanical properties of PVA film added with BA have been improved, which showed a very promising application in biomedical materials. Therefore, this experiment further improves the thermal stability and mechanical properties of the film by adding BA, which can enable the film to obtain a wider range of applications.
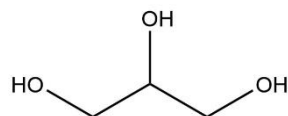
Figure 7. Glycerol

2. Experimental section

2.1. Materials

SRC extracted from the seaweed Eucheuma cottonii was purchased from W-Hydrocolloids, Inc. Philippines; PVA (PL032, Degree of Hydrolysis 86 - 90%, Mw<100,000) was purchased from Chem-supply Pty Ltd. Australia; Glycerol (molecular weight of 92.09 g /mol) was purchased from Sigma Aldrich Australia; CIN (natural >95%, Mw=132.16) was purchased from Sigma Aldrich Australia; BA(AR grade, Mw =61.83g/mol)was purchased from Merck Pty Ltd Australia; Milli-Q water was used as the solvent in the film preparations.

2.2. Film preparation

Disperse the SRC in Milli-Q water at a concentration of 0.02 g/ml. After dissolving at room temperature, the mixture was heated to 80°C-90°C in a magnetic stirrer and stirred for 15 minutes. The hot solution was then poured onto a glass plate and allowed to gel at room temperature for 30 min and heated in an oven at 60-70 °C for 1 day to dry. The rationale for heating the solution of a concentration of 0.02 g/mL at 80-90°C for 15 minutes is to ensure that SRC exists in dilute solution form in water and simultaneously avoid moisture evaporation and ensure complete reaction. This is the preparation of pure SRC film. PVA was dispersed in Milli-Q water at a concentration of 0.04 g/mL, it was heated at and stirred until complete dissolution. Then the same procedure as the pure SRC film. Glycerol (gly) as shown in Figure 7, 40 % with respect to SRC, was added to the mixture as plasticizer. PVA 33 % with respect to SRC, was added as reinforcing agent. BA 10 % with respect to SRC, was dispersed in Milli-Q water at a concentration of 0.01 g/mL as acidic environment provider. CIN, 10 % with respect to SRC, was added directly to the mixture as crosslinker.The composition of the formulation for this experiment is shown in Table 1.

Table 1. The formula composition of this experiment

sample	content	mass ratio
Formula 1	SRC powder	100
Formula 2	SRC /glycerol film	100/40
Formula 3	SRC / glycerol/CIN film	100/40/10
Formula 4	SRC / glycerol/ BA film	100/40/10
Formula 5	PVA film	33.3
Formula 6	PVA/ BA film	33.3/10
Formula 7	SRC /glycerol/PVA film	100/40/33.3
Formula 8	SRC /glycerol/PVA/CIN	100/40/33.3/10
Formula 9	SRC / glycerol/PVA/CIN/BA	100/40/33.3/10/10

The mixture solution was also heated at 80°C-90°C and stirred to ensure complete reaction.

2.3. Film structural characterization

Fourier Transform Infrared Spectroscopy (FTIR)was used to characterize the presence of specific chemical groups in the materials. Very thin films were obtained and analysed by PerkinElmer FTIR Spectrometer Frontier. The sample was cut to the size of 10 mm × 10 mm and the film thickness was measured using a smart thickness gauge, and a film with a thickness of 40 μm was selected for

measurement. It was measured in the attenuated total reflectance mode in the wave number range of 4000 to 600^{-1}, 32 scans per test. Results were recorded in duplicate. Data were analyzed using OMNIC software and plotted using Origin software.

DSC analysis was done by Mettler-Toledo DSC1 STAR system. Samples were weighted into standard aluminium pans. A sealed empty pan was used as reference material while nitrogen gas was purged at 20 ml/min during experiments. Each sample was carried out with temperature ranging from 60°C to 300°C at scanning rate of 10 °C/min.

XRD patterns were recorded at room temperature on a rigaku mini flex 600 diffraction system, using Cu Kα (λ = 1.5406 Å) radiation. The sample is cut into 10mm x 10mm size and adhered to the plate, then placed on the sample holder of the diffractometer. The samples analysis over 2θ covered a range of 2° - 70° with a sampling interval of 0.02°. The scan speed is 2°/min. Data were analyzed using Jade software and plotted using Origin software.

2.4. Film properties measurement

The mechanical properties of the films were measured by using an Instron Universal Testing Instrument (Model 4465) with a 5 kN load cell. The films were cut into strips (100 mm × 15 mm) and their Tensile Strength (TS) and percent elongation at break (EB) were measured. An initial gauge length of 50 mm and a cross-head speed of 10 mm/ min were used for each sample. A minimum of five strips of film (10 × 1.5 cm) were measured for each sample to obtain an average value for each of the measured properties.

3. Results and discussion

3.1. FTIR characterization analysis of modified films

FT-IR spectra are used to detected the changes in hydroxyl groups in material structure. Table 2 showed the peak positions corresponding to the movement of hydroxyl groups [24]. From 3650cm^{-1} to2500cm^{-1} denotes the stretching vibration of hydroxyl groups. From 1275cm^{-1} to 1000cm^{-1} denotes the stretching vibration of carbonyl groups.

Table 2. Characteristic peak of hydroxyl group

Hydroxyl type	O-H, ν	C-O(H), ν
Free hydroxyl group	3650-3580	1275-1000
Primary alcohol	3650-3630	1075-1000
Secondary alcohol	3635-3620	1130-1030
Tertiary alcohol	3620-3600	1210-1100
Phenol	3610-3590	1275-1150
Intermolecular association	3550-3200	——
Intramolecular association	3600-2500	——
Crystal water	3600-3100	——
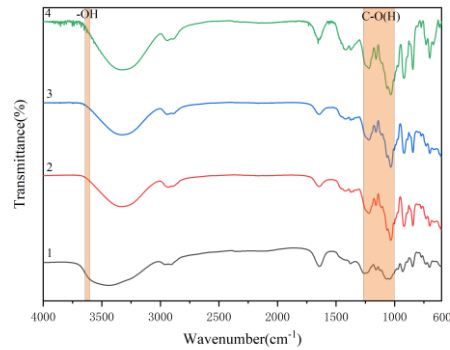
(a) SRC powder and films
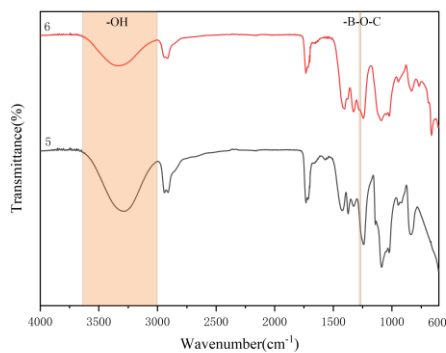
(b) PVA films
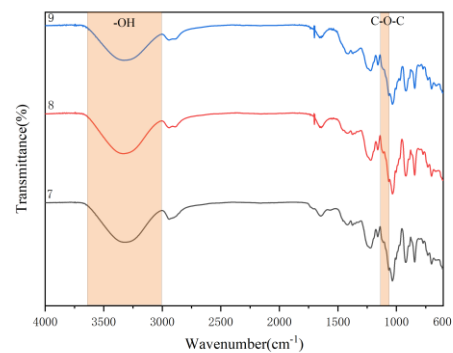
(c) SRC/PVA blend films

Figure 8. FT-IR spectra for various film samples

From Figure 8 (a), curve1 is the FT-IR spectra of SRC powder, only the primary and secondary hydroxyl groups of SRC are present in the structure. Curve2 is the spectra of SRC film plasticized with glycerol, the tertiary alcohol groups of glycerol, the intermolecular and intramolecular associations caused by hydration shift the peak height to the right. Compared with Curve2, Curve 3 and Curve 4 show sharper and higher peak at $1275 cm^{-1}$ $-1000 cm^{-1}$, it can be inferred that the products of the structures in Figure 4 and Figure 6 have been generated. More carbonyl groups are reflected in the FT-IR spectra.

From Figure 8 (b), compared with curve 5 of pure PVA film, curve 6 exhibited a new broad peak at $1290 cm^{-1}$-$1270 cm^{-1}$, corresponding to the stretching vibrations of B-O-C [25]. Moreover, the intensity of the peak at $3650 cm^{-1}$-$3000 cm^{-1}$ (the stretching vibration of hydroxyl groups of PVA) in modified PVA films was reduced. This can be attributed to the structural changes that occur during the crosslinking reaction, where the free -OH groups interact with BA, thereby changing the hydrogen-bonded hydroxyl group.

From Figure 8 (c), comparing the three curves of SRC/PVA blend films, the reduced intensity of the peak at $3650 cm^{-1}$-$3000 cm^{-1}$ and the strong absorption peaks at $1150 cm^{-1}$ -$1060 cm^{-1}$ (the stretching vibrations of aliphatic ether C-O-C) [26] means that high conversion rate of acetal reaction occurred in the present of BA(curve 9).

3.2. XRD characterization analysis of modified films

Calculated crystallinity of related samples

sample	crystallinity
Formula 1	12.53%
Formula 2	11.71%
Formula 3	7.66%
Formula 4	11.88%
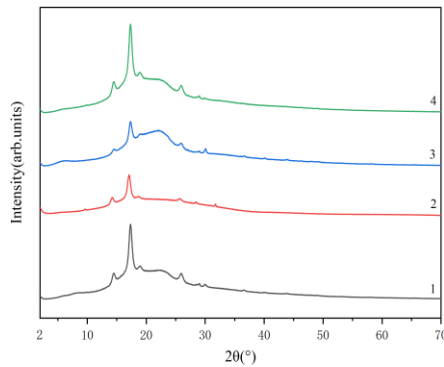
(a) SRC powder and films

Calculated crystallinity of related samples

sample	crystallinity
Formula 5	28.64%
Formula 6	10.79%
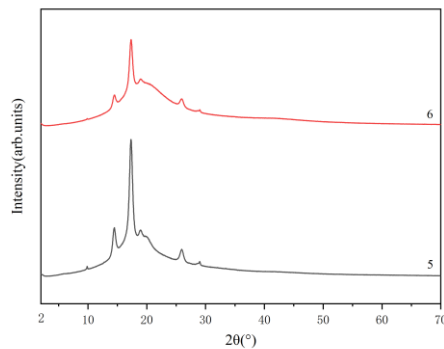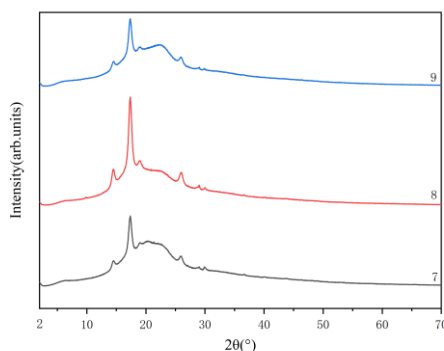
(b) PVA based films

Calculated crystallinity of related samples

sample	crystallinity
Formula 7	5.69%
Formula 8	18.68%
Formula 9	6.86%

(c) SRC/PVA blend films

Figure 9. XRD spectra for various film samples

Figure 9 shows the XRD spectra of various thin films and the crystallinity of various thin films obtained through Jade software fitting analysis. The analysis of the crystallinity of the film provides side evidence of the cross-linking of the film. The restriction of molecular rearrangement after cross-linking leads to a decrease in crystallinity. The crystallinity of SRC is the three-dimensional regular structure of SRC, calculated based on the same principle as crystallinity. It is calculated by the following equation:

$$Xc = \frac{A_{crystal}}{A_{crystal} + A_{amorph}}$$

where $A_{crystal}$ is the area of the crystalline region and A_{amorph} is the area of the non-crystalline region.

From the XRD spectrum of SRC powder and films in Figure 9 (a), there are obvious diffraction peaks at 14.2 °, 17 °, and 18.6 ° [27]. Crystallinity calculation results indicate that plasticizing (Formula 2), adding CIN (Formula 3) and adding BA (Formula 4) fully reduced the crystallinity of the film, especially CIN. The acetal reaction with SRC did not show significant structural changes in XRD spectrum, but only disrupted the degree of crystal regularity of SRC.

In the XRD spectrum of Figure 9 (b), both curves are at 2θ= 17.3 ° displays the typical characteristic peak of PVA. The film of PVA added with BA (Formula 6) has the low crystallinity than pure PVA (Formula 5)film which indicate the same reason as SRC [28].

According to Figure 9(c), the crystallinity of SRC and PVA decreased after simple blending (Formula 7) because of the formation of a large number of hydrogen bonds that disrupt their original regular structures. After adding CIN (Formula 8), the crystallinity increased, which may be due to CIN as an heterogeneous nucleating agent increasing the crystallization in the PVA membrane [29] Formula 9 indicated that under acidic conditions of BA, there was a marked drop in crystallinity which also be attributed to chemical reactions.

3.3. Thermodynamic characterization analysis of modified films

The DSC curves at the second temperature rise measured at a temperature rise of 10°C/min are shown in Figure 10 and the calculated results are listed in Table 3.
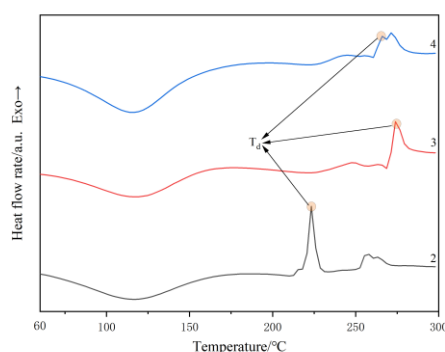
(a) SRC- based films
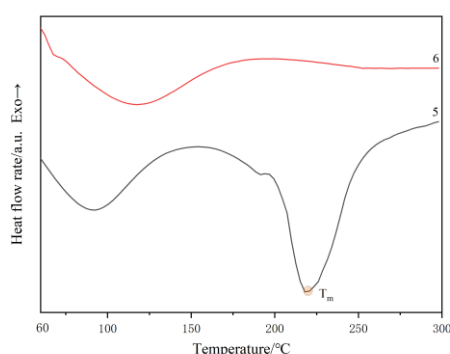
(b) PVA-based films
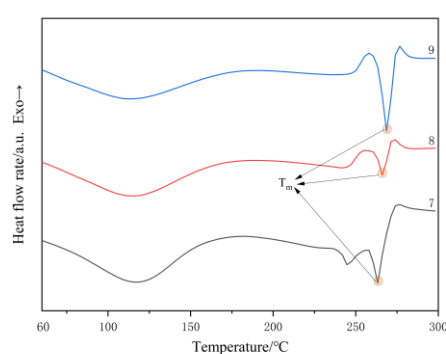
(c) SRC/PVA blend films

Figure 10. DSC thermal curve of heating trend of various film samples

From Figure 10 (a), it can be seen that all samples exhibit exothermic peaks (T_d) at 210-280 °C, which corresponds to the cleavage of glycosidic bonds. The exothermic peak shifts towards a higher temperature, which may be due to the formation of chemical bonds between the additive and SRC. Based

on the data in Table 3, in the first three formulas, the addition of CIN results in a relatively high T_g and T_d values for SRC film.

In Figure 10 (b), pure PVA (Formula 5) has a melting peak (T_m) at around 218℃, which is formed by the melting of the crystalline portion of PVA and the heat absorbed by the decomposition of a small amount of PVA molecules. After adding BA (Formula 6), the T_g increase and the T_m almost disappears, which respectively corresponding to the stability of molecular structure caused by H-bonding and the less melting of crystalline phase [30].

According to Figure 10 (c) and Table 3, comparing three blending formulas, T_g and Tm continues to rise. This increase in thermal stability may be due to the acetal structure formed in the film [31].

Table 3. Thermal properties for various film samples

sample	DSC		
	Glass transition point $T_{g\,(℃)}$	Endothermic peak temperature T_m (℃)	Exothermic peak temperature T_d (℃)
Formula 2	138.2	——	233
Formula 3	144.4	——	274
Formula 4	139.2	——	266
Formula 5	111.3	218	——
Formula 6	121.4	——	——
Formula 7	139.1	263	——
Formula 8	140.2	266	——
Formula 9	145.5	268	——

3.4. Characterization and analysis of mechanical properties of modified films

Preparing casting films of various modified ingredients and preparing tensile specimens according to the requirements of 2.4, the result of TS and EB of the films were shown in Figure 11.

(a)   (b)   (c)
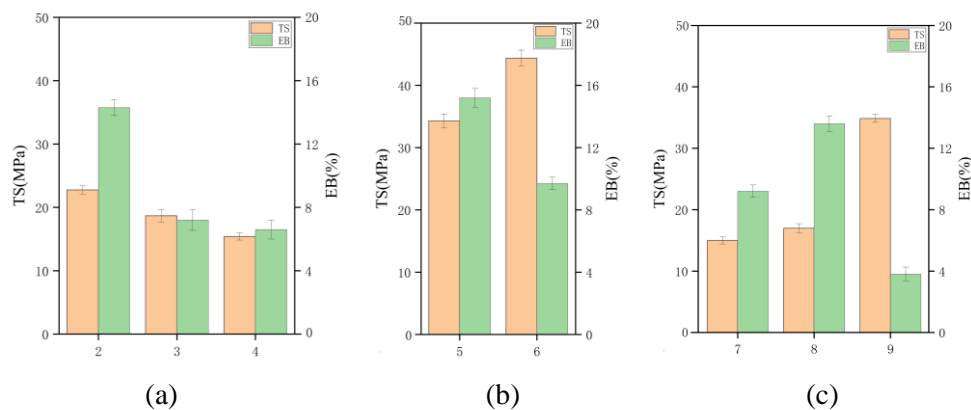
Figure 11. Comparison Chart of Different Tensile Strength and Elongation at break Values

From Figure 11 (a), it appears that, compared to the plasticized SRC film, the addition of CIN and BA reduces the TS and EB of the modified film, but the mechanical properties of the film with BA

decrease more significantly, which is related to the incomplete molecular interaction formed and is consistent with the previous microscopic analysis.

Figure 11 (b) shows a comparison of the mechanical properties of films between pure PVA and PVA added with BA. It can be seen that the addition of BA increases the TS and EB. And the thermal analysis in Table 3 shows an increase in heat resistance after the addition of BA, which is consistent with the mechanical property data and serves as a unified verification. Based on the infrared spectrum analysis in Figure 8 (b), it can be inferred that the acetal reaction of BA forms a stable cross-linking network structure with the hydroxyl groups of linear PVA, enhancing the rigidity of the material and reducing its ductility.

Figure 11(c) shows a comparison of the mechanical properties of the SRC/PVA blend films using different additives. It can be seen that formulation 9 with CIN and BA acting together has the highest TS value and the lowest EB value compared to the pure carrageenan film and the pure PVA film. Sedayu [27] used sodium benzoate solution as a photosensitizer to photocrosslink the surface of semi-refined carrageenan (SRC) film samples with UV light, and the EB values of the prepared cross-linked films were significantly lower than those of the control. This is the same trend as that obtained for the cross-linked membranes in this experiment. The infrared spectrum analysis of Figure 8 (c) verifies that under the acidic conditions provided by BA, CIN has the highest probability of acetal reaction with SRC and PVA, resulting in high cross-linking degree, denser cross-linking network, and high macroscopic performance low toughness. The crystallinity analysis in Figure 9 (c) verified the decrease in crystallinity of the blend caused by cross-linking, while the thermal analysis in Table 3 showed an improvement in the heat resistance of the cross-linked structure, which is consistent with the mechanical property data and plays a unified role in verification. Compared with formulas 7 and 9, formula 8 lacks an acidic environment and has a low degree of acetalization of CIN, forming a loose network structure. Macroscopically, it exhibits a higher EB value. Compared to formula 2 and formula 5, formula 7 indicates that the mechanical properties of SRC/PVA blend films with simple blending are lower than those of plasticized SRC films and PVA films, indicating poor compatibility and lack of synergistic effect between these two resins.

4. Conclusions

Due to the difficulty of casting pure SRC into a film, compared with pure SRC powder, the microstructure of several formulas of modified SRC films prepared through the casting process in an aqueous solution at 80°C-90°C are investigated. The micro-characterization methods include infrared spectroscopy, XRD and DSC. The changes of molecular structure, crystallinity and thermal properties of the films are analysed respectively. The macroscopic mechanical properties are characterized by tensile experiments of constant thickness films.

The results indicate that from a macro perspective, the mechanical properties of plasticized carrageenan film and modified carrageenan film with additive are not as good as those of PVA film and modified PVA film. So PVA resin used as a blending modifier for SRC films. Under the mass ratio of SRC/glycol/PVA/CIN/BA=100/40/33/10/10, both microscopic and macroscopic analyses have shown that under the acidic conditions of BA, SRC undergoes acetal reaction with PVA and CIN, resulting in a tensile strength of 34.85 MPa and an elongation at break of only 3.8% for the prepared film. The formula without adding BA has a low incidence of acetal reaction, a tensile strength of 16.96 MPa, and an elongation at break of 13.6%. Its mechanical properties are superior to those of simple blend films.

This research provides a new approach and idea for developing high-performance SRC packaging films, which can effectively improve the tensile strength and other properties of SRC films, thus expanding their application scope and market share in food packaging. In the future, the addition of CIN and BA can be adjusted within a certain range according to the requirements of stiffness and toughness, and the ratio of acetal and cross-link density can be adjusted under a microscope. As an environmentally friendly and biodegradable material, they can be applied in the food packaging industry. There are still limitations in this study, as carrageenan is very hydrophilic, resulting in slow drying of cross-linked films, and the fast drying of carrageenan-modified films can be a research direction in the future.

References

[1] Azizi S, Mohamad R, Abdul Rahim R, Mohammadinejad R and Bin Ariff A 2017 Hyd rogel beads bio-nanocomposite based on Kappa-Carrageenan and green synthesized silver nanoparticles for biomedical applications *Int J Biol Macromol* **104** 423–31

[2] Necas J and Bartosikova L 2013 Carrageenan: a review *Vet. Med.* **58** 187–205

[3] Kanmani P and Rhim J-W 2014 Development and characterization of carrageenan/grapefruit seed extract composite films for active packaging *Int J Biol Macromol* **68** 258–66

[4] Sedayu B B, Cran M J and Bigger S W 2020 Improving the moisture barrier and mechanical properties of semi-refined carrageenan films *J Appl Polym Sci* **137** 49238

[5] Sedayu B B, Cran M J and Bigger S W 2020 Reinforcement of Refined and Semi-Refined Carrageenan Film with Nanocellulose *Polymers* **12** 1145

[6] Khan M A, Hussain Z, Liaqat U, Liaqat M A and Zahoor M 2020 Preparation of PBS/PLLA/HAP Composites by the Solution Casting Method: Mechanical Properties and Biocompatibility *Nanomaterials* **10** 1778

[7] Abdul Khalil H P S, Banerjee A, Saurabh C K, Tye Y Y, Suriani A B, Mohamed A, et al. 2018 Biodegradable Films for Fruits and Vegetables Packaging Application: Preparation and Properties *Food Eng Rev* **10** 139–53

[8] Thakur R, Pristijono P, Golding J B, Stathopoulos C E, Scarlett C, Bowyer M, et al. 2018 Effect of starch physiology, gelatinization, and retrogradation on the attributes of rice starch-ι-carrageenan film *Starch - Stärke* **70** (1-2) 1700099

[9] Jiang J-L, Zhang W-Z, Ni W-X and Shao J-W 2021 Insight on structure-property relationships of carrageenan from marine red algal: A review *Carbohyd Polym* **257** 117642

[10] Daei S, Mohtarami F and Pirsa S 2022 A biodegradable film based on carrageenan gum/Plantago psyllium mucilage/red beet extract: physicochemical properties, biodegradability and water absorption kinetic *Polym. Bull.* **79** 11317–38

[11] Sedayu B B, Cran M J and Bigger S W 2019 A Review of Property Enhancement Techniques for Carrageenan-based Films and Coatings *Carbohyd Polym* **216** 287–302

[12] Rhim J-W and Wang L-F 2014 Preparation and characterization of carrageenan-based nanocomposite films reinforced with clay mineral and silver nanoparticles *Appl Clay Sci* **97–98** 174–81

[13] Chan M-K and Tang T-H 2022 The properties of starch/cellulose/polyvinyl alcohol composite as hydrodegradable film *Polym Polym Compos* **30** 096739112211003

[14] Yang D, Liu Q, Gao Y, Wan S, Meng F, Weng W and Zhang Y 2023 Characterization of silver nanoparticles loaded chitosan/polyvinyl alcohol antibacterial films for food packaging *Food Hydrocolloid* **136** 108305

[15] Kazeminava F, Javanbakht S, Nouri M, Adibkia K, Ganbarov K, Yousefi M, Ahmadi M, Gholizadeh P and Kafil H S 2022 Electrospun nanofibers based on carboxymethyl cellulose/polyvinyl alcohol as a potential antimicrobial wound dressing *Int J Biol Macromol* **214** 111–9

[16] Schiessl S, Kucukpinar E, Cros S, Miesbauer O, Langowski H-C and Eisner P 2022 Nanocomposite Coatings Based on Polyvinyl Alcohol and Montmorillonite for High-Barrier Food Packaging *Front Nutr* **9** 790157

[17] Bajpai S K, Dehariya P and Saggu S P S 2015 Investigation of Moisture Sorption, Permeability, Cytotoxicity and Drug Release Behavior of Carrageenan/Poly Vinyl Alcohol Films *J Macromol Sci A* **52** 243–51

[18] Tanaka T, Lu T, Yuasa S and Yamaura K 2001 Structure and properties of poly(vinyl alcohol)/κ-carrageenan blends *Polym Int* **50** 1103–8

[19] Friedman M 2017 Chemistry, Antimicrobial Mechanisms, and Antibiotic Activities of Cinnamaldehyde against Pathogenic Bacteria in Animal Feeds and Human Foods *J Agric Food Chem.* **65** 10406–23

[20] Gao H and Yang H 2021 Preparation and characterization of cinnamaldehyde/polyvinyl alcohol/silver nanoparticles ternary composite films *Int J Polym Anal Ch* **26** 24–36

[21] Lim M, Kwon H, Kim D, Seo J, Han H and Khan S B 2015 Highly-enhanced water resistant and oxygen barrier properties of cross-linked poly(vinyl alcohol) hybrid films for packaging applications *Prog Org Coat* **85** 68–75

[22] Şenel M, Bozkurt A and Baykal A 2007 An investigation of the proton conductivities of hydrated poly(vinyl alcohol)/boric acid complex electrolytes *Ionics* **13** 263–6

[23] Prosanov I Yu, Bulina N V and Gerasimov K B 2013 Complexes of polyvinyl alcohol with insoluble inorganic compounds *Phys Solid State* **55** 2132–5

[24] Snyder R W, Painter P C, Havens J R and Koenig J L 1983 The Determination of Hydroxyl Groups in Coal by Fourier Transform Infrared and 13C NMR Spectroscopy *Appl Spectrosc* **37** 497–502

[25] Park K, Oh Y, Panda P K and Seo J 2022 Effects of an acidic catalyst on the barrier and water resistance properties of crosslinked poly (vinyl alcohol) and boric acid films *Prog Org Coat* **173** 107186

[26] Li S, Luo C, Tang F, Xiao W, Fang M, Sun J and Chen W 2022 Effect of polyethylene glycol modified MWCNTs-OH on the crystallization of PLLA and its stereocomplex *J Polym Res* **29** 162

[27] Sedayu B B, Cran M J and Bigger S W 2021 Effects of surface photocrosslinking on the properties of semi-refined carrageenan film *Food Hydrocolloid* **111** 106196

[28] Ren Y, Tian T, Jiang L, Liu X and Han Z 2018 Polyvinyl Alcohol Reinforced Flame-Retardant Polyacrylonitrile Composite Fiber Prepared by Boric Acid Cross-Linking and Phosphorylation *Materials* **11** 2391

[29] Gao H 2018 PhD in Construction and Sustained Release Control of Cinnamaldehyde/Polyvinyl Alcohol Antibacterial Packaging Film System (Shaanxi University of Science and Technology)

[30] Park J-S, Park J-W and Ruckenstein E 2001 On the viscoelastic properties of poly(vinyl alcohol) and chemically crosslinked poly(vinyl alcohol) *J Appl Polym Sci* **82** 1816–23

[31] Distantina S, Rochmadi R, Fahrurrozi M and Wiratni W 2013 Preparation and Characterization of Glutaraldehyde-Crosslinked Kappa Carrageenan Hydrogel *Eng J* **17** 57–66